applied sciences

MDPI

Article

Model-Based Analysis of Different Equivalent Consumption Minimization Strategies for a Plug-In Hybrid Electric Vehicle

Stefan Geng [1,2,*], Thomas Schulte [1] and Jürgen Maas [2]

[1] iFE—Institute for Energy Research, OWL University of Applied Sciences and Arts, Campusallee 12, 32657 Lemgo, Germany; thomas.schulte@th-owl.de
[2] Mechatronic Systems Laboratory, Faculty of Mechanical Engineering and Transport Systems, Technical University of Berlin, Hardenbergstraße 36, 10623 Berlin, Germany; juergen.maas@tu-berlin.de
* Correspondence: stefan.geng@campus.tu-berlin.de

Abstract: Plug-in hybrid electric vehicles (PHEVs) are developed to reduce fuel consumption and the emission of carbon dioxide. Common powertrain configurations of PHEVs (i.e., the configuration of the combustion engine, electric motor, and transmission) can be operated either in series, parallel, or power split hybrid mode, whereas powertrain configurations with multimode transmissions enable switching between those modes during vehicle operation. Hence, depending on the current operation state of the vehicle, the most appropriate mode in terms efficiency can be selected. This, however, requires an operating strategy, which controls the mode selection as well as the torque distribution between the combustion engine and electric motor with the aim of optimal battery depletion and minimal fuel consumption. A well-known approach is the equivalent consumption minimization strategy (ECMS). It can be applied by using optimizations based on a prediction of the future driving behavior. Since the outcome of the ECMS depends on the quality of this prediction, it is crucial to know how accurate the predictions must be in order to obtain acceptable results. In this contribution, various prediction methods and real-time capable ECMS implementations are analyzed and compared in terms of the achievable fuel economy. The basis for the analysis is a holistic model of a state-of-the-art PHEV powertrain configuration, comprising the multimode transmission, corresponding powertrain components, and representative real-world driving data.

Keywords: PHEV; ECMS; multimode transmission; optimization; powertrain modeling

Citation: Geng, S.; Schulte, T.; Maas, J. Model-Based Analysis of Different Equivalent Consumption Minimization Strategies for a Plug-In Hybrid Electric Vehicle. *Appl. Sci.* **2022**, *12*, 2905. https://doi.org/10.3390/app12062905

Academic Editor: Daniela Anna Misul

Received: 14 February 2022
Accepted: 8 March 2022
Published: 11 March 2022

1. Introduction

Today, vehicle manufacturers are forced to reduce the fuel consumption of their products because of enhanced environmental regulations. A promising solution is the development of plug-in hybrid electric vehicles (PHEV), as they combine an extended electric cruising range and the possibility of propelling the vehicle by an internal combustion engine (ICE) when the battery is depleted or when high performance is required. Common powertrain configurations of PHEVs are the series, parallel, and power split configurations. The efficiencies of these configurations vary depending on the distance and the power demand of the intended trip [1]. Increased efficiency can be obtained by using so-called multimode or dedicated hybrid transmissions (DHTs). This type of transmission enables switching between different powertrain configurations during vehicle operation and combining the individual advantages of these configurations. A general property of a DHT is that the electric motors are an integral and indispensable part of the transmission [2], which is the case when only the electric motor is able to propel the vehicle in a certain speed range. Since the part of the transmission for the ICE can be designed for the remaining and, in general, smaller speed range, a DHT requires fewer speeds and is less complex in comparison with a conventional automatic transmission. This saves a part of the additional weight and installation space caused by the electrification of the vehicle. Examples of available PHEVs equipped with a DHT can be found in [3–7].

Figure 1 shows the basic concept of a hybrid electric powertrain with a DHT, which is abstractly considered a configuration of two clutches (C), a transmission (T) with a constant gear ratio i_{ED}, a planetary gear (PG) with a stationary gear ratio i_0, and a two-speed transmission (2ST) with the gear ratios $i_{1/2}$. The concept requires only one electric drive and enables a continuous variable transmission mode (CVT), a parallel hybrid mode (PAR), and an electric driving mode (EM), where each mode can be driven in two speeds due to the two-speed transmission at the output. Clutch C_1 connects the ICE to the DHT, and clutch C_2 blocks the planetary gear (i.e., all shafts of the planetary gear rotate with the same speed). In this case, the speed ratios between the transmission's output and the two input shafts are constant and depend on the state of C_1 when either the parallel hybrid or the electric driving mode are active. Due to the chosen transmission ratios, the parallel hybrid mode can only be driven at higher vehicle speeds. Otherwise, the rotational speed of the ICE will fall below its lower limit, and the engine will stall. To operate the vehicle at lower speeds, the electric driving mode or, if the battery is discharged, the CVT mode must be activated. In this mode, the rotational speeds of the ICE and electric motor are superimposed by a planetary gear, whereby the speed of the ICE can be adjusted continuously as a function of the speed of the electric motor and the final drive. The design of the transmission ratios ensures that the electric motor operates as a generator in CVT mode until an appropriate vehicle speed is reached. A more detailed description can be found in a previous work [8], where the basic concept was used for the development of a new DHT including a specific configuration of gears and clutches and the corresponding transmission ratios.

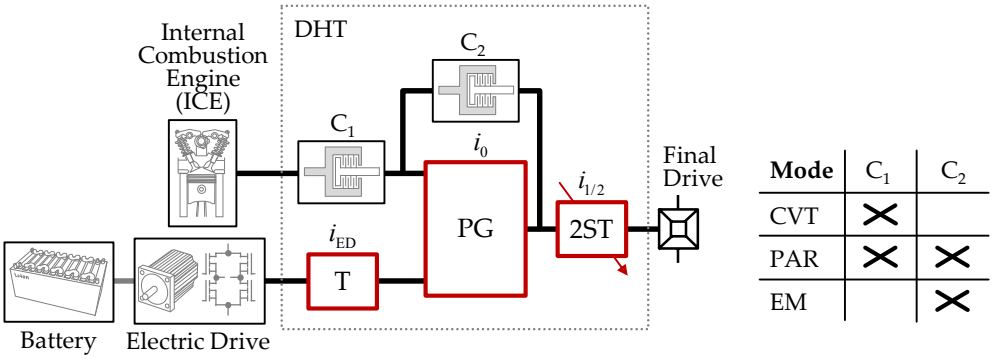

Figure 1. Basic concept of a hybrid electric powertrain with a DHT.

The operation of the hybrid electric powertrain requires an appropriate operating strategy, which determines the operation mode of the DHT and the torque distribution between the ICE and electric motor with the aim of maximal fuel economy. According to [9–11], numerous approaches for implementing such strategies are already known and classified into heuristic and optimization-based methods. Figure 2 shows an overview of the commonly applied methods.

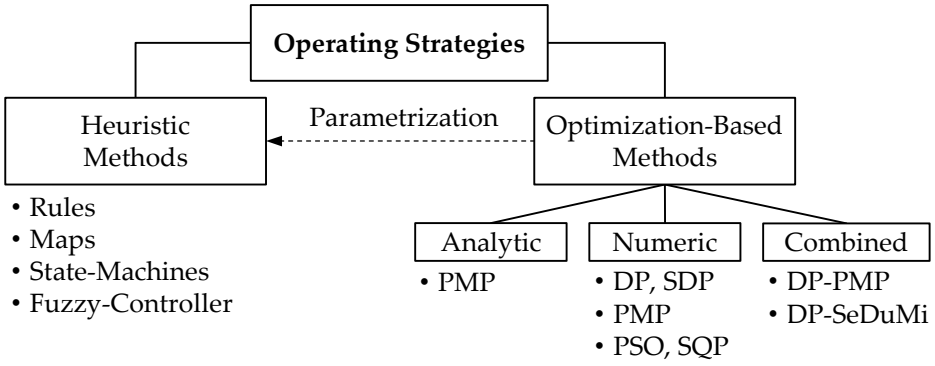

Figure 2. Classification of operation strategies for hybrid electric vehicles.

Heuristic operating strategies are implemented as simple rules, maps [12–14], state machines, or fuzzy controllers [15–17], where the parametrization is frequently carried out based on the experience of the powertrain's developers and adjusted by means of empirical studies and test driving. It often aspires to reduce fuel consumption by shifting all operating points of the vehicle to an efficient operating area of the ICE. Since the operation of the electric motor is not taken into account optimally, optimal operation in terms of minimal fuel consumption is not possible. A further approach for parametrization is to incorporate the results from an optimization-based method, which is performed using representative driving cycles [18–20] (see dotted arrow in Figure 2).

Usually, heuristic methods provide only suboptimal results, since the parametrization is based on predefined assumptions without considering real driving behavior. Due to this disadvantage, it is generally not possible to obtain the minimal possible fuel consumption. However, the main advantage is the simplicity of the method's implementation, which makes it suitable for real-time application on a vehicle's electronic control units. Moreover, no information on future driving behavior must be known in advance in order to operate the vehicle.

Optimization-based methods provide optimal results in terms of fuel economy. Here, fuel consumption is defined to be a cost function, which is minimized for a given driving cycle by using a mathematical optimization. In general, these methods require a powertrain model in order to describe the fuel consumption, depending on the vehicle's operating point. For this purpose, map-based models are frequently used, where the fuel consumption of the ICE and the energy efficiency of the electric drive are considered by means of corresponding maps. When using map-based powertrain models, only numerical optimization methods can be applied. Typical numerical methods for optimization-based operating strategies proposed in the literature are Dynamic Programming (DP) [21,22], Stochastic Dynamic Programming (SDP) [23], Pontryagin's Maximum Principle (PMP) [24,25], Particle Swarm Optimization (PSO) [26], and Sequential Quadratic Programming (SQP) [27]. Another approach is to use an analytic powertrain model, where the maps are approximated by convex functions [28]. These functions are often simple polynomials and enable solving the optimization problem of the operating strategy analytically by means of PMP [29–31]. However, the application is restricted to continuous control variables (e.g., the torque distribution between ICE and the electric drive). In [32], the analytical optimization with PMP was combined with DP in order to consider the gear-shifting command as a discrete control variable. For the same powertrain configuration and control problem, in [33], a combination of DP and an optimization based on interior point methods using the SeDuMi tool was applied on a convex powertrain model.

The advantage of an operating strategy based on mathematical optimization is that it provides minimal fuel consumption. However, a driving cycle must be known in advance, and some of the methods require high computational effort. Therefore, these methods are inapplicable for real vehicle operation but are appropriate for powertrain analyses and optimizations.

For real driving operation, real-time capable operating strategies are required. An overview of various methods can be found in [34,35]. Optimization-based methods are preferred in general, since they consider information about the future driving behavior and consequently provide better results than heuristic methods. Since the exact driving behavior is unknown, and due to unforeseeable driving styles and traffic situations, predictions are used (e.g., based on telemetry data). Well-known real-time capable operating strategies are the Equivalent Consumption Minimization Strategy (ECMS) [35–37] and various Model Predictive Control (MPC) approaches [38–40], while the optimization-based implementation of the ECMS is equivalent to PMP [41].

In this contribution, different implementations of the optimization-based EMCS algorithm are analyzed in terms of the theoretically achievable fuel economy. These implementations are based on different approaches for predicting the future driving cycle, while the accuracy of the predictions increases with the prediction effort and the quality of the

predicted information. For the analysis, the hybrid electric powertrain given by the basic concept shown in Figure 1 is used. All implementations of the ECMS are evaluated by means of corresponding powertrain simulations, which are carried out with representative real-world driving data as the input.

Therefore, in Section 2, the powertrain model used for implementing and evaluating the optimization-based ECMS is presented. The control of the hybrid electric powertrain by means of the ECMS requires the definition of an optimization problem and a method for its solution. Both are described based on the previously defined powertrain model in Section 3 and are applied in Section 4, comprising the ECMS algorithm and the different prediction methods. Finally, in Section 5, the results of the powertrain simulations considering various ECMS implementations are evaluated and discussed.

2. Powertrain Model

The ECMS implementation is based on a powertrain model, which is used to perform a local optimization in order to determine the powertrain's control signals. Since the optimization needs to be applied in real time, a powertrain model with low computational effort and yet a sufficient level of detail is required. This is obtained by the so-called backward approach [42]. Starting with the requested acceleration a_{veh} and speed v_{veh} of the vehicle, the operating states of each powertrain component are determined backwards (see Figure 3). A vehicle dynamics model determines the required torque T_{FD} and angular velocity ω_{FD} at the final drive. In order to satisfy these requirements, the DHT model determines the corresponding torques and angular velocities of the ICE and electric drive considering the transmission's control variables s_{m} and u_{ED}. It is always assumed that the ICE and the electric drive are capable of generating the required torque and satisfying the requested vehicle acceleration, respectively. The submodels of the DHT, ICE, electric drive, and battery consider stationary states only, as no controllers are required to operate these components. Only the operation mode of the powertrain must be controlled via the DHT. Therefore, s_{m} defines the mode (CVT, PAR, or EM mode) and u_{ED} the torque or angular velocity of the electric drive, definable due to the resulting degree of freedom in the PAR and CVT modes, respectively. Both control variables are determined by the ECMS and are considered here as inputs of the powertrain model. Since no dynamic behavior is considered, the operation mode changes immediately without any transition (e.g., continuously changing the state of a clutch from engaged to disengaged). The output of the powertrain simulation is the mass flow rate of the fuel $\dot{m}_{\mathrm{f}}$ and the state of charge of the battery SoC.

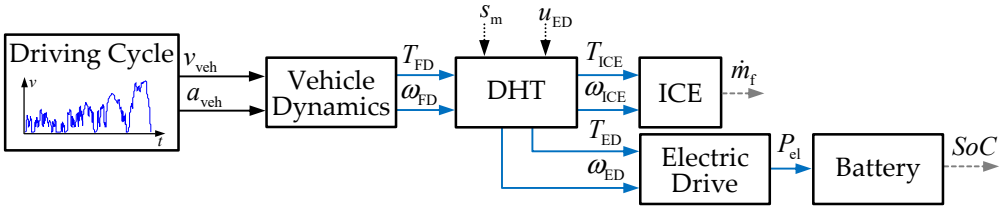

Figure 3. Powertrain model according to the backward approach and the basic concept shown in Figure 1.

Figure 4 shows the submodels of the powertrain and their most significant parameters. The models of the ICE and electric drive are map-based, whereby only the state behavior of the components is considered. To determine the specific fuel consumption b_{e} and power loss $P_{\mathrm{ED,loss}}$, the corresponding torques and speeds are used.

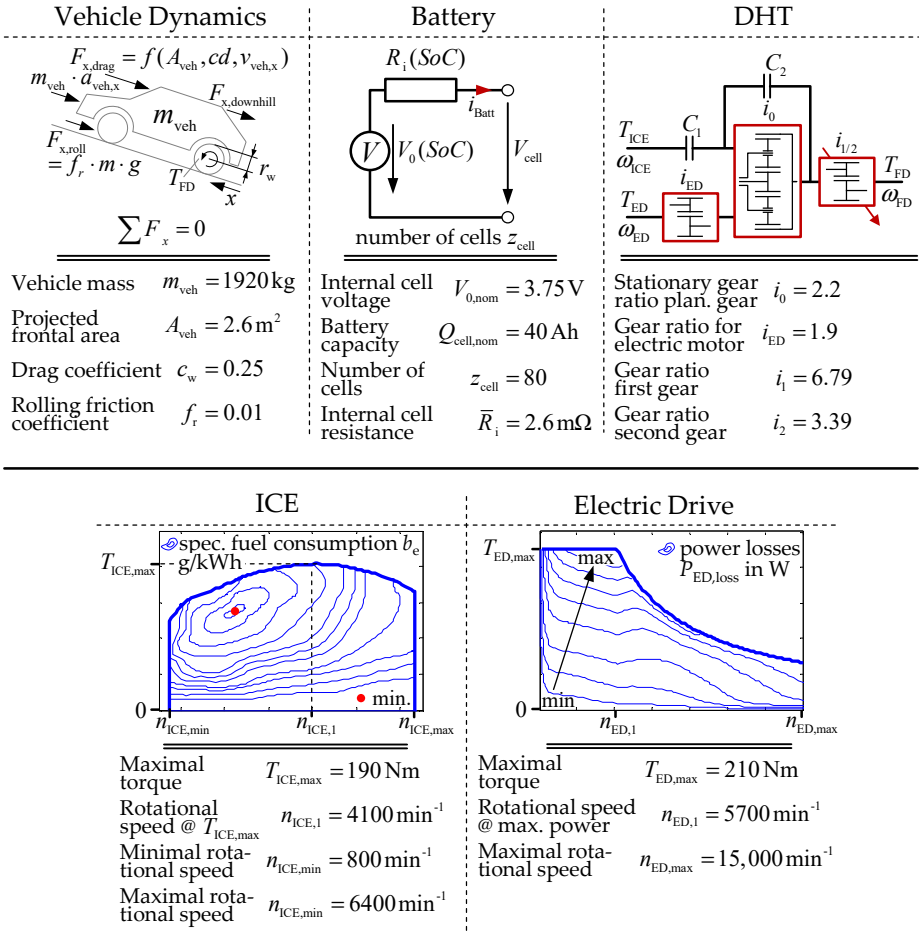

Figure 4. Models of the powertrain components and the most important parameters.

The vehicle dynamics are considered in a longitudinal direction only. The torque T_{FD} and angular velocity ω_{FD} at the final drive are determined according to the following equation:

$$T_{FD} = r_w \cdot \left(F_{drag}(v_{veh}) + F_{roll} + F_{downhill} + m_{veh} \cdot a_{veh} \right), \quad (1)$$

with the radius of the wheels r_w, the vehicle mass m_{veh}, the vehicle speed v_{veh}, and the vehicle acceleration a_{veh} (extracted from the driving cycle). The forces represent the driving resistances comprising the drag force F_{drag}, the rolling friction force F_{roll}, and the downhill force $F_{downhill}$. In order to consider the inertias of the wheels and the flywheel mass of the ICE, equivalent masses are added to the overall vehicle mass. In the case of the flywheel mass, the average transmission ratio is used for parameter conversion.

By means of the torque T_{FD} and the rotational speed ω_{FD} at the final drive, the model of the DHT is evaluated (i.e., the torques and rotational speeds of the ICE and the electric drive are determined by considering the operation mode):

$$s_m = \begin{cases} j & \text{for CVT-Mode in } j\text{-th gear,} \\ j+2 & \text{for PAR-Mode in } j\text{-th gear,} \\ j+4 & \text{for EM-Mode in } j\text{-th gear,} \end{cases} \quad (2)$$

where j denotes the gear in which the corresponding mode is driven. Since a two-speed transmission is considered, each operation mode can be driven in two speeds ($j \in \{1, 2\}$).

Furthermore, the control variable for the electric drive u_{ED} is defined according to current operation state s_{m} and the corresponding degree of freedom:

$$u_{\mathrm{ED}} = \begin{cases} \omega_{\mathrm{ED}} & \text{for } s_{\mathrm{m}} = 1 \ldots 2, \\ T_{\mathrm{ED}} & \text{for } s_{\mathrm{m}} = 3 \ldots 4, \\ f(T_{\mathrm{FD}}, \omega_{\mathrm{FD}}) & \text{for } s_{\mathrm{m}} = 5 \ldots 6. \end{cases} \tag{3}$$

In the case of the EM mode, no degree of freedom exists, and consequently, T_{ED} and ω_{ED} are completely defined by means of the torque and angular velocity at the final drive. The model of the DHT comprises a simple planetary gear model with the stationary gear ratio i_0. Its sun gear is connected to the ICE, its ring gear to the electric drive, and its carrier to the two-speed transmission. Considering this configuration as well as the transmission ratios of the two-speed transmission i_j and the electric drive i_{ED}, the torques and angular velocities in the CVT mode are determined according to the following equation:

$$\begin{aligned} T_{\mathrm{ED}} &= -i_0 \cdot \left((1+i_0) \cdot i_{\mathrm{ED}} \cdot i_j\right)^{-1} \cdot T_{\mathrm{FD}}, \\ T_{\mathrm{ICE}} &= \left((1+i_0) \cdot i_j\right)^{-1} \cdot T_{\mathrm{FD}}, \\ \omega_{\mathrm{ICE}} &= (1+i_0) \cdot i_j \cdot \omega_{\mathrm{FD}} + i_0 \cdot i_{\mathrm{ED}}^{-1} \cdot \omega_{\mathrm{ED}}, \end{aligned} \tag{4}$$

with the angular velocity of the electric drive ω_{ED} as the degree of freedom ($u_{\mathrm{ED}} = \omega_{\mathrm{ED}}$). Analogously, the angular speeds and torques in the PAR mode can be derived, yielding the following:

$$\begin{aligned} \omega_{\mathrm{ED}} &= -i_{\mathrm{ED}} \cdot i_j \cdot \omega_{\mathrm{FD}}, \\ \omega_{\mathrm{ICE}} &= i_j \cdot \omega_{\mathrm{FD}}, \\ T_{\mathrm{ICE}} &= i_j^{-1} \cdot T_{\mathrm{FD}} + i_{\mathrm{ED}} \cdot T_{\mathrm{ED}}, \end{aligned} \tag{5}$$

where the torque of the electric drive T_{ED} needs to be chosen ($u_{\mathrm{ED}} = T_{\mathrm{ED}}$). For the EM mode, only the torque and angular velocity of the electric drive must be determined:

$$\begin{aligned} T_{\mathrm{ED}} &= -\left(i_{\mathrm{ED}} \cdot i_j\right)^{-1} \cdot T_{\mathrm{FD}}, \\ \omega_{\mathrm{ED}} &= -i_{\mathrm{ED}} \cdot i_j \cdot \omega_{\mathrm{FD}}. \end{aligned} \tag{6}$$

The ICE is represented by a map, which describes the specific fuel consumption b_{e} as a function of the torque T_{ICE} and rotational speed ω_{ICE}. The mass flow rate of the fuel is determined according to the following equation:

$$\dot{m}_{\mathrm{f}} = \frac{b_{\mathrm{e}}(T_{\mathrm{ICE}}, \omega_{\mathrm{ICE}}) \cdot T_{\mathrm{ICE}} \cdot \omega_{\mathrm{ICE}}}{3.6 \cdot 10^6}, \tag{7}$$

with $\dot{m}_{\mathrm{f}}$ in $\mathrm{g \cdot s^{-1}}$. Similarly, the required electric power P_{el} of the electric drive is determined by

$$P_{\mathrm{el}} = T_{\mathrm{ED}} \cdot \omega_{\mathrm{ED}} + P_{\mathrm{ED,loss}}(|T_{\mathrm{ED}}|, |\omega_{\mathrm{ED}}|), \tag{8}$$

where the power loss $P_{\mathrm{ED,loss}}$ represents the result of the corresponding map, shown in Figure 4. This map also includes the power losses of the inverter. Since the electric power P_{el} must be provided by the battery, the battery current is expressed as

$$\dot{q} = -i_{\mathrm{Batt}} = -\frac{V_0(SoC)}{2 \cdot R_{\mathrm{i}}(SoC)} + \sqrt{\left(\frac{V_0(SoC)}{2 \cdot R_{\mathrm{i}}(SoC)}\right)^2 - \frac{P_{\mathrm{el}}}{z_{\mathrm{cell}} \cdot R_{\mathrm{i}}(SoC)}}. \tag{9}$$

This follows from the simplified equivalent circuit in Figure 4, where z_{cell} is the number of cells, V_0 is the internal cell voltage, and R_{i} is the internal cell resistance. In

this representation, V_0 and R_i are functions of the state of charge, considering the nominal battery capacity $Q_{cell,nom}$:

$$SoC = \frac{100}{3600} \cdot \int \frac{\dot{q}}{z_{cell} \cdot Q_{cell,nom}} dt. \tag{10}$$

Since the powertrain model is executed in discrete time steps, the integration of $\dot{q}$ can be solved explicitly (i.e., no algebraic loop occurs).

Next, the powertrain model described above is used for the optimal control of the considered hybrid electric powertrain. Furthermore, it is part of the ECMS implementation presented in Section 4.

3. Optimal Control of the Hybrid Electric Powertrain

The criterion for optimal control of the hybrid electric powertrain is minimal fuel consumption (i.e., for a given driving cycle, the electric drive and the ICE must be operated in such a way that the consumed fuel is minimal). Therefore, the mass flow rate of the fuel $\dot{m}_f$ in Equation (7) is defined to be a cost function, while the overall costs and fuel consumption are obtained by integrating $\dot{m}_f$ over the duration of the driving cycle t_e:

$$m_f = \int_0^{t_e} \dot{m}_f(T_{ICE}, \omega_{ICE}) dt. \tag{11}$$

Additionally, the battery current is expressed as

$$\dot{q} = -i_{Batt}(q, P_{el}), \tag{12}$$

with the following initial and end conditions:

$$\begin{aligned} q_0 &= \tfrac{SoC_0}{100} \cdot z_{cell} \cdot Q_{cell,nom}, \\ q_e &= \tfrac{SoC_e}{100} \cdot z_{cell} \cdot Q_{cell,nom}, \end{aligned} \tag{13}$$

which are related to the battery's state of charge at the beginning SoC_0 and the end SoC_e of the driving cycle that must be considered. The evaluation of the state of Equation (12) requires the electrical power P_{el}, which is consumed or generated by the electrical drive. According to Equation (8), it can be summarized as

$$P_{el} = f_{ED}(T_{ED}, \omega_{ED}). \tag{14}$$

The torques and angular velocities of the ICE and electric drive in Equations (11) and (14) are determined by the transmission model of Equations (2)–(6). This can be summarized as follows:

$$[T_{ICE}\ T_{ED}\ \omega_{ICE}\ \omega_{ED}]^T = f_{Trans}(T_{FD}, \omega_{FD}, \mathbf{u}), \tag{15}$$

with the torque T_{FD} and angular velocity ω_{FD} at the final drive resulting from the vehicle dynamics model in Equation (1) and the control variable of the powertrain:

$$\mathbf{u} = \begin{bmatrix} s_m \\ u_{ED} \end{bmatrix}. \tag{16}$$

It must be taken into account that the control variable as well as the state variable are limited due to the technical boundaries of the powertrain components:

$$\begin{aligned} &s_m \in \mathcal{U}_T, && \text{with } \mathcal{U}_T = \{s_m \in \mathbb{N} | 1 \le s_m \le 6\}, \\ &u_{ED} \in \mathcal{U}_{ED}, && \text{with } \mathcal{U}_{ED} = \left\{u_{ED} \in \mathbb{R} \middle| u_{ED} \in \mathcal{U}_{T_{ED}} \text{ or } u_{ED} \in \mathcal{U}_{\omega_{ED}}\right\}, \\ &q \in \mathcal{X}_q, && \text{with } \mathcal{X}_q = \{q \in \mathbb{R} | 0 \le q \le z_{cell} \cdot Q_{cell,nom}\}. \end{aligned} \tag{17}$$

The sets $\mathcal{U}_{T_{ED}}$ and $\mathcal{U}_{\omega_{ED}}$ correspond to the torque and angular velocity boundaries, respectively, given by the maps of the ICE and electric drive shown in Figure 4. In order to obtain the optimal control of the hybrid electric powertrain, the minimal fuel consumption

$$m_f^* = \min_{\mathbf{u}} m_f(\mathbf{u}) \tag{18}$$

must be determined with respect to Equations (11)–(17). The optimal control variable $\mathbf{u}^*$ is a result of Equation (18).

In general, the various methods for the solution of the optimization problem in Equations (11)–(18) are known. One approach is Pontryagin's Maximum Principle (PMP). It is based on variational calculus and the enhancement of considering the boundaries of the control variables in Equation (17). For obtaining the optimal control variable $\mathbf{u}^*$ by means of PMP, the Hamilton function

$$\mathcal{H}(\lambda, \mathbf{u}, q) = -\dot{m}_f(\mathbf{u}) + \lambda \cdot \dot{q}(\mathbf{u}, q) \tag{19}$$

must be evaluated while considering the necessary conditions given in [43]. In Equation (19), λ is the Lagrange multiplier. If it is known in advance, the optimal control variable $\mathbf{u}^*$ will be obtained by finding the maximum of the Hamilton function with respect to Equations (11)–(17):

$$\mathcal{H}^* = \max_{\mathbf{u}} \left\{ -\dot{m}_f(\mathbf{u}) + \lambda \cdot \dot{q}(\mathbf{u}, q) \right\}. \tag{20}$$

Usually, the Lagrange multiplier λ is a function of time and the vehicle's position such that Equation (20) can be carried out as a local optimization for a certain position of the vehicle. In the EMCS algorithm, the control variables of the powertrain are determined by means of this local optimization, where λ is obtained by a prediction (see Section 4).

Another method for solving the optimization problem in Equations (11)–(18) is based on Dynamic Programming (DP). Here, the driving cycle is separated into discrete instants of time $t_k = k \cdot T$, with the step size T and $k = 0 \dots N$. Additionally, the state and input variables are quantized by means of the state variable grid $\mathbf{q}^g = [q_1^g \dots q_n^g]^T$ and the input variable grids $\mathbf{s}_m^g = [\mathbf{s}_{m,1}^g \dots \mathbf{s}_{m,o}^g]^T$ and $\mathbf{u}_{ED}^g = [u_{ED,1}^g \dots u_{ED,m}^g]^T$. A cost matrix $\mathbf{J}$ with n rows and N columns defines the accumulated costs for all possible state transitions from one time step to another. Each row is assigned to the corresponding state within $\mathbf{q}^g$ and each column to the instant of time t_k. In order to obtain $\mathbf{J}$, a backward computation beginning with $k = N - 1$ and ending with $k = 0$ is carried out. In each time step k, the minimal costs must be determined for all $i = 1 \dots n$ as follows:

$$J_{i,k} = \min_{\mathbf{u}_k} \left\{ J_{p,k+1} + T \cdot \dot{m}_f(\mathbf{u}_k) \right\}. \tag{21}$$

The minimum is determined by evaluating all possibilities for the control variable $\mathbf{u}_k$ (i.e., all combinations of the elements within the grid vectors $\mathbf{s}_m^g$ and $\mathbf{u}_{ED}^g$ with respect to the system boundaries defined in Equation (17). For the determination of the costs $J_{p,k+1}$, the state equation is evaluated:

$$q_p = q_i^g + T \cdot \dot{q}\left(\mathbf{u}_k, q_i^g\right), \tag{22}$$

where the index p denotes the row in $\mathbf{q}^g$ of $\mathbf{J}$ assigned to q_p. Since q describes a continuous variable, it might not match an element within the predefined state grid $\mathbf{q}^g$. In this case, $J_{p,k+1}$ is interpolated based on the surrounding elements within $\mathbf{q}^g$ [21].

Once the cost matrix $\mathbf{J}$ is known, the optimal control variable $\mathbf{u}^*$ is obtained by means of a forward computation beginning with $k = 0$ and ending with $k = N - 1$:

$$\mathbf{u}_k^* = \arg\min_{\mathbf{u}_k} \left\{ J_{p,k+1} + T \cdot \dot{m}_f(\mathbf{u}_k) \right\}, \tag{23}$$

where $J_{p,k+1}$ is determined analogously to the backward computation based on the following state equation:

$$q_p^* = q_k^* + T \cdot \dot{q}(\mathbf{u}_k, q_k^*). \tag{24}$$

Here, the optimal electric charge q_k^* and beginning with q_0^* relate to the initial state of charge SoC_0 (see Equation (13)). Since DP can only be applied on a driving cycle, which is known in advance, it cannot be used as a real-time capable operating strategy. Furthermore, a very high computation effort is required when choosing a high resolution for the state and input variable grids. Nevertheless, DP can be used to predict λ for the ECMS and to compute the theoretically minimal fuel consumption for a given driving cycle. The latter is used as an optimum serving as reference for the evaluation of the results obtained by the ECMS algorithm.

4. Equivalent Consumption Minimization Strategy (ECMS)

In this section, the ECMS algorithm will be presented. It is based on the powertrain models presented in Section 2 and the optimization methods presented before. Figure 5 shows the algorithm of the ECMS. The input variables are the current state of charge SoC_k, the vehicle speed $v_{\mathrm{veh},k}$, and the vehicle acceleration $a_{\mathrm{veh},k}$. Considering an implementation adapted to the real vehicle operation, SoC_k and $v_{\mathrm{veh},k}$ are measured values, and $a_{\mathrm{veh},k}$ is a request from the driver. However, for the intended analysis, $a_{\mathrm{veh},k}$ as well as $v_{\mathrm{veh},k}$ were obtained from a driving cycle and the SoC_k from a powertrain model. The ECMS algorithm is based on PMP and carries out a local optimization of the Hamilton function (Equation (19)) in each time step. In order to evaluate the Hamilton function, the powertrain model (Equations (1)–(10)) was used to determine the fuel consumption and battery current for a given control variable $\mathbf{u}_k$. Furthermore, the Lagrange multiplier λ_k was required, representing a function of the current state of charge SoC_k and position of the vehicle $z_{\mathrm{veh},k}$. This function was obtained from a prediction of the future driving behavior, which had to be carried out in advance. For the optimization of the Hamilton function, the control variable $\mathbf{u}_k$ was quantized by means of the grid vectors $\mathbf{s}_{\mathrm{m}}^{\mathrm{g}}$ and $\mathbf{u}_{\mathrm{ED}}^{\mathrm{g}}$ (see Section 3).

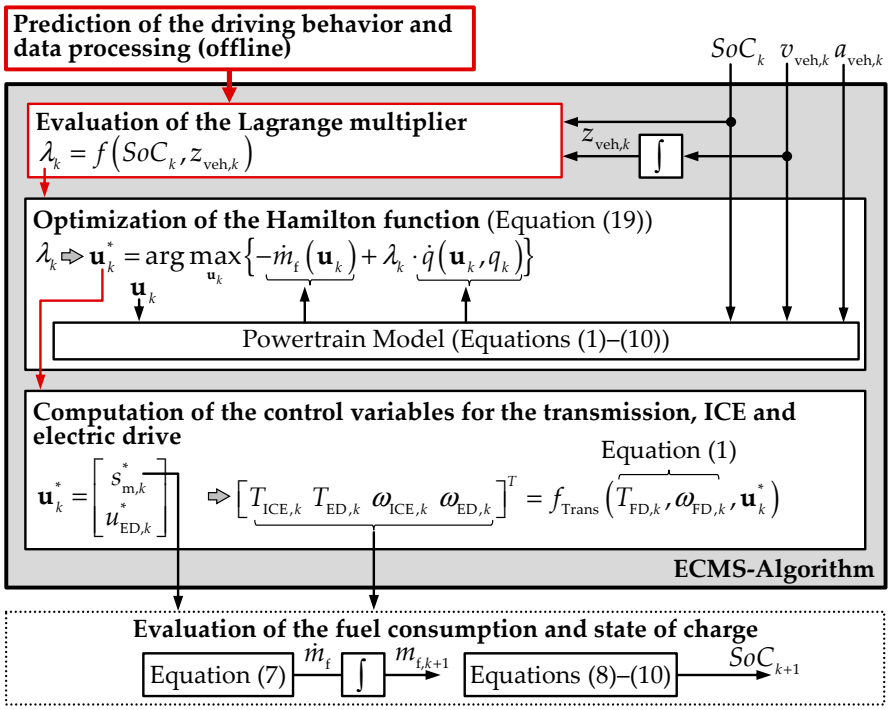

Figure 5. Implemented ECMS algorithm based on PMP with a prediction of the future driving behavior and the evaluation of the overall fuel consumption and the state of charge.

This enabled finding the maximum by testing all possible combinations given by the grid vectors. In general, it is possible to apply other methods to obtain the optimum, but it must be ensured that the correct solution is found and the computation time of the ECMS algorithm is still adequate. Once the control variable $\mathbf{u}_k^*$ was known, it was used to evaluate the torques and angular velocities of the ICE and electric drive by means of the transmission model (Equations (4)–(6)). For real vehicle operation, these values as well as the transmission control variable $\mathbf{s}_\mathrm{m}^*$ were the setpoints for the controllers of the corresponding powertrain components. Here, these values were used to determine the fuel consumption $m_{\mathrm{f},k+1}$ and state of charge SoC_{k+1} by means of the same powertrain model, which was already applied to the optimization.

Crucial for obtaining good results with the ECMS is a well-chosen Lagrange multiplier λ_k matching the real driving behavior as well as possible. Since the real driving behavior was unknown in advance, λ_k was obtained by means of a prediction. For this purpose, two already known methods from the literature were considered in this contribution. These methods are presented in the following subsections.

4.1. Method 1: Hamilton–Jacobi–Bellman Equation

The Lagrange multiplier λ_k required for evaluating the ECMS algorithm can be obtained by means of DP in Equations (21)–(24). Due to the high computational effort of DP, it must be precomputed based on a driving cycle. This driving cycle can only be predicted and needs to approximate the future driving behavior as well as possible. In order to determine λ_k, the Hamilton–Jacobi–Bellman equation is used [43]:

$$\frac{\partial J^*(q,t)}{\partial t} = \max_{\mathbf{u}} \{ -\dot{m}_\mathrm{f}(\mathbf{u}) \underbrace{- \frac{\partial J^*(q,t)}{\partial q}}_{\lambda} \cdot \dot{q}(\mathbf{u},q) \}. \tag{25}$$

This equation describes the connectedness between the DP and PMP, where the right side represents the Hamilton function (Equation (19)). Accordingly, the partial derivative of the optimal accumulated costs J^* from the battery charge q corresponds to λ. Due to the discrete functional principle of DP, the partial derivative must be approximated by the following means for $k = 0 \ldots N-1$ and $i = 1 \ldots n$:

$$\lambda_{i,k} = -\frac{J_{i+1,k} - J_{i,k}}{q_{i+1}^\mathrm{g} - q_i^\mathrm{g}}. \tag{26}$$

The states q_i^g correspond to the elements within the state variable grid $\mathbf{q}^\mathrm{g} = [q_1^\mathrm{g} \ldots q_\mathrm{n}^\mathrm{g}]^T$ used for carrying out DP and the costs $J_{i,k}$ for the elements within the cost matrix $\mathbf{J}$, describing the result of the backward computation (Equation (21)). Since each index k is assigned to an instant of time t_k, it can be also assigned to a vehicle position $z_{\mathrm{veh},k}$ by integrating the vehicle speeds $v_{\mathrm{veh},k}$ given by the considered driving cycle. Moreover, the elements in the state variable grid $\mathbf{q}^\mathrm{g}$ can be converted into a state of charge according to Equation (10). Consequently, from Equation (26), λ is the result of a function of $z_{\mathrm{veh},k}$ and SoC_k, as shown in Figure 5.

Figure 6 shows an example for the Lagrange multipliers λ determined according to Equation (26). The upper figure shows λ as a function of z_veh and SoC. It also contains the optimal characteristics of the state of charge SoC^* for the initial values $SoC_0 = 80\%$ (red line) and $SoC_0 = 30\%$ (green line). Both characteristics were the result of DP, which was applied on the same driving cycle used to determine λ. The lower figure shows the Lagrange multipliers λ belonging to SoC^*. Both characteristics were obtained from the upper diagram. If the battery is constantly discharged during vehicle operation, the values for λ will be lower than if the state of charge is kept constant or the battery is charged. In the algorithm of the ECMS shown in Figure 5, the function for λ is implemented as a map, which corresponds to the upper part of Figure 6.

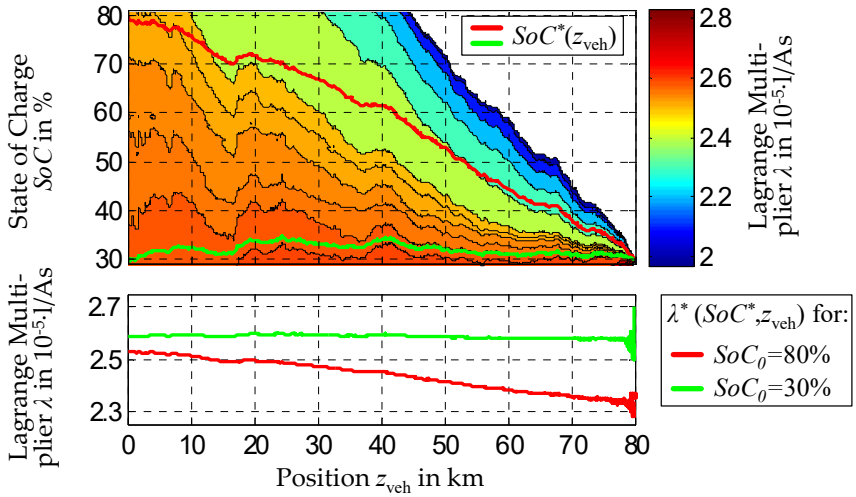

Figure 6. The Lagrange multiplier λ as a function of the state of charge *SoC* and the vehicle's position z_{veh}, determined by the Hamilton–Jacobi–Bellman equation (Equation (25)).

4.2. Method 2: PI Controller

The second investigated method for obtaining the Lagrange multiplier is a feedback control, where λ is used to control the *SoC* [35,44] (see Figure 7). A PI controller is used, since the integrating part enables initializing λ to a value within an appropriate range (see Figure 6). In addition, the dynamic behavior of λ can be influenced by means of the time constant and gain of the controller. If the current state of charge SoC_k falls below the setpoint SoC_k^{SP}, the PI controller increases λ_k, and the battery charges. Otherwise, λ_k will be decreased, and the battery discharges (compare Figure 6). The parameters of the PI controller are determined empirical in such a way that the initial λ_0 is chosen appropriately, and an oscillating behavior of λ_k is almost avoided. Due to this, frequent changes in the transmission speeds and modes during vehicle operation are avoided.

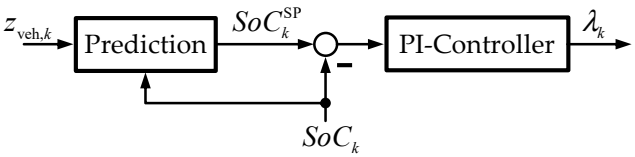

Figure 7. Control of the *SoC* with the control variable λ and predicted setpoints SoC^{SP}.

The setpoints for the controller SoC^{SP} are the result of a predicted function, which describes the state of charge as a function of the current vehicle position $z_{\text{veh},k}$. For this purpose, the three approaches shown in Figure 8 are considered. Figure 8a shows a linear discharge characteristic, beginning with the initial state of charge at the start position and ending with the lower boundary of the state of charge at the end position of the trip. For this kind of prediction, only the distance of the intended trip to be driven is required. In Figure 8b, the linear discharge characteristic is adapted when the state of charge exceeds the current characteristic due to recuperating the braking energy. This adaptation is carried out in every execution step of the ECMS algorithm. The last approach for the prediction, shown in Figure 8c, is based on an optimized discharge characteristic, which is obtained by applying DP on a predefined driving cycle. As in the case of the Hamilton–Jacobi–Bellmann equation presented in the previous section, this kind of prediction requires a representative driving cycle and time-consuming optimization in advance.

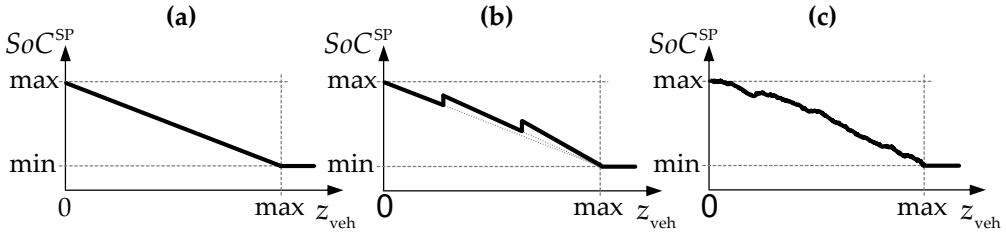

Figure 8. Prediction of SoC^{SP}: (**a**) linear characteristic, (**b**) linear characteristic with adaptation to the recuperated braking energy, and (**c**) optimized characteristic obtained from DP for a predicted driving cycle.

The method based on the Hamilton–Jacobi–Bellmann equation as well as the control-based method can be used for the determination of the Lagrange multiplier required for the ECMS algorithm shown in Figure 5. In order to apply one of these methods, either a driving cycle or the distance of the intended trip must be predicted. In the following section, the ECMS is applied by means of both methods. Each ECMS implementation is applied on different predictions and is analyzed in terms of the resulting fuel consumptions.

5. Analysis of Different ECMS

For the analysis of the ECMS, the fuel consumptions obtained by applying the different prediction methods described in Section 4 were compared to each other. The powertrain model was parametrized according to Figure 4, while the evaluation of the fuel consumptions was carried out according to the ECMS algorithm shown in Figure 5. In the simulation, the vehicle braked by means of recuperation, which was limited to a maximal electrical power of 35 kW. Furthermore, the battery's initial state of charge was defined to be 80%, and the lower boundary was set to 30%.

In order to consider the difference between the predictions and the real driving behavior, various driving cycles of the same route were simulated. For this purpose, a daily commute in both directions was measured 39 times, including sections on a German interstate. Each of these driving cycles had a distance of 80 km and was unique due to varying driving behavior and traffic. Figure 9 shows the minimal, maximal, and mean vehicle speeds resulting from the measured driving cycles. Additionally, a driving cycle of the same route obtained from the navigation data is shown. This driving cycle as well as the mean driving cycle was used for the predictions, while the measured driving cycles were used to evaluate the fuel consumptions.

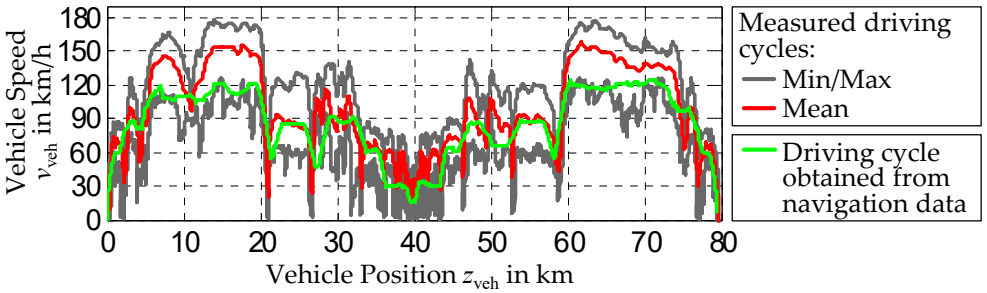

Figure 9. Minimal, maximal, and mean value of 39 measured driving cycles of the same route and the route's driving cycle obtained from navigation data [45].

Figure 10 shows the simulation results obtained from the ECMS for all considered prediction methods and driving cycles. For comparison, the results of an offline optimization with DP (black marker) are shown, representing the theoretically minimal fuel consumption for each of the measured driving cycles. Furthermore, the results of a simple CD-CS operating strategy (charge depleting–charge sustaining) are shown, too (grey marker). It was first driven with the electric motor until the battery reached its lower boundary of the state of

charge. Then, it was mainly driven by the ICE, keeping the state of charge constant. The CD-CS strategy was applied by means of the control-based approach, where $SoC^{SP} = 30\%$ was a constant setpoint. The results of the 39 driving cycles were arranged in ascending order of energy for propulsion so that the fuel consumptions on the left corresponded to a conservative driving style and those on the right corresponded to an agile driving style.

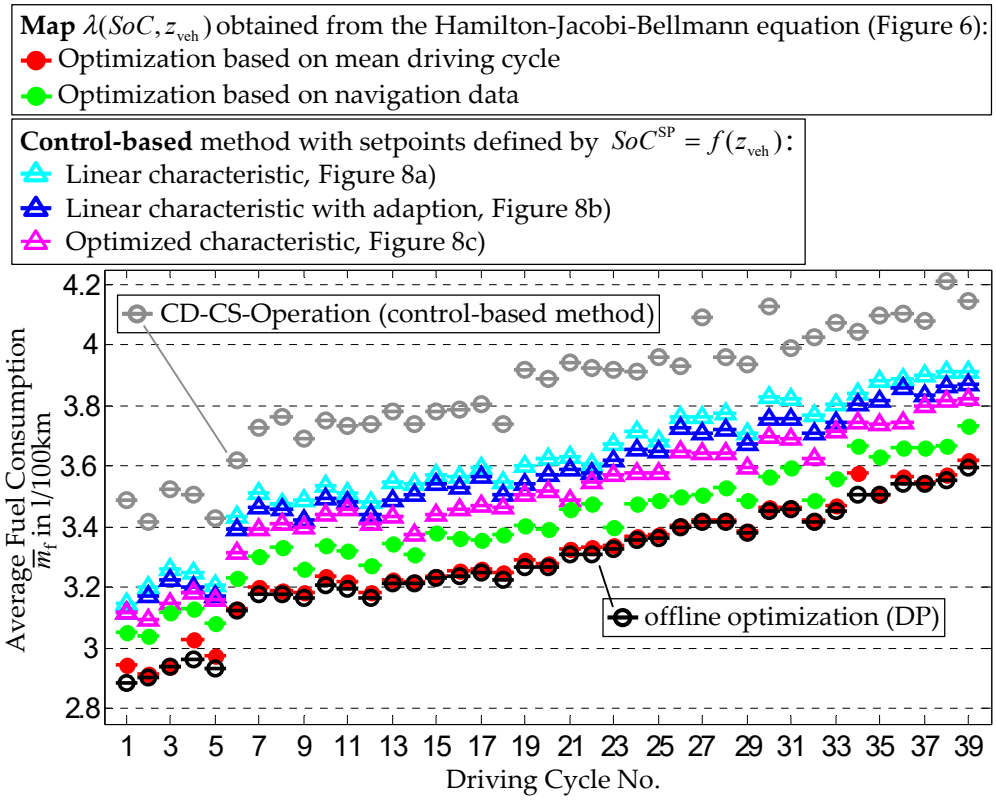

Figure 10. Simulation results for the ECMS, showing average fuel consumptions for all driving cycles and prediction methods.

The lowest fuel consumptions were obtained by the ECMS based on the Hamilton–Jacobi–Bellmann equation (red marker), where the mean driving cycle was used for parametrization. However, since such a driving cycle is generally unknown, it can only be determined when the driving behavior of frequently driven routes is measured (e.g., daily commute). More common is the parametrization according to the navigation data (green marker), which does not need any measurements and causes slightly higher fuel consumptions. For the application of both ECMS variants, a representative driving cycle must be determined, and in particular, a time-consuming optimization needs to be carried out in advance. Therefore, it is rather appropriate for trips, which can be scheduled in advance.

The fuel consumptions obtained by applying the control-based methods were generally higher compared with the consumptions obtained with the method based on the Hamilton–Jacobi–Bellmann equation. As expected, the best results were obtained with an optimized state of charge characteristic for the setpoints of the controller (purple marker). This variant also required a predefined driving cycle and optimization in advance, which was carried out here by means of DP. However, it was basically possible to apply another optimization method, which enabled faster computation of the state of charge characteristic (e.g., the combination of DP and PMP [32]. In comparison with the approach based on the Hamilton–Jacobi–Bellmann equation, the control-based approach had the potential to be initialized faster. The other variants (blue and cyan marker) only required the distance of the intended trip in order to define the characteristic for the setpoints of the controller. Adapting this characteristic to the current state of charge when recuperating (blue marker)

enabled slightly lower fuel consumptions. This, however, depended on how much energy could be recuperated. Since these variants did not require a driving cycle or optimization in advance, it was also possible to apply them to instantaneous trips.

Table 1 shows an overview of the considered operating strategies and the corresponding information required for its applications. Furthermore, it contains the mean percentage increase of the fuel consumptions obtained by each operating strategy related to the theoretically minimal fuel consumption obtained with DP. The results show that only minor information about the driving cycle enabled the ECMS to achieve significantly lower fuel consumptions compared with the non-optimization-based CD-CS operation. In addition, the more information about the future driving cycle was available, the lower the fuel consumptions obtained by the ECMS were. Optimization-based predictions led to an improvement in the results, while the best results were obtained when the real driving behavior was used for optimization. The control-based method with a linear characteristic required the same input information as the control-based method with the adaption to the *SoC* but caused higher fuel consumption. For this reason, it was more beneficial to apply the variant with the adaption, since the additional implementation effort was only slightly increased. The variant with the optimized characteristic further reduced the fuel consumption but required optimization in advance. The advantage in comparison with the method based on the Hamilton–Jacobi–Bellmann equation is that the optimization does not need to be carried out with DP. Another optimization method can be chosen which computes the required characteristic significantly faster (e.g., the method presented in [32]).

Table 1. Overview of the considered operating strategies and summary of the simulation results shown in Figure 10.

Operating Strategy	Prediction Method	Input Information	Deviation to Minimal Fuel Consumption [1] ( )
ECMS based on the Hamilton-Jacobi-Bellmann equation	Optimization results from DP (map)	Averaged driving cycle of the real driving behavior	0.6% ( )
		Driving cycle from navigation data	3.8% ( )
ECMS with control-based method	Optimization results from DP [2] (Optimized characteristic *SoC**)	Averaged driving cycle of the real driving behavior	6.9% ( )
	Linear characteristic with adaption to the current *SoC*	Distance of the intended route	8.7% ( )
	Linear characteristic		10.1% ( )
CD-CS-Operation	-	-	17.4% ( )

[1] Mean percental increase of the fuel consumptions obtained with each operating strategy related to the theoretically minimal fuel consumptions obtained with the DP. [2] Not necessarily DP, as the optimized characteristic can also be obtained by means of other optimization methods.

Since the ECMS was applied for the same model used for the ECMS algorithm itself, some of the resulting fuel consumptions were very close to the theoretical minimum. In practice, however, the powertrain model used for the ECMS algorithm differed from the real powertrain (e.g., due to neglecting the powertrain dynamics) so that, in reality, higher fuel consumptions were to be expected. Nevertheless, it can be assumed that the previously identified tendencies of reducing the fuel consumptions by improving the prediction methods will still remain.

The required input information can be obtained by using the intended route information of the navigation system, providing the driver's needs. Furthermore, automatized approaches are recommended for recognizing and logging frequently driven routes.

6. Conclusions

This contribution described a model-based analysis of different ECMS implementations for a plug-in hybrid electric powertrain, which can be operated in different operation modes and each of them operating at two speeds. A corresponding powertrain model was

developed based on the backward simulation approach. This model neglects the system dynamics except for the vehicle mass and describes the fuel and energy consumptions by means of maps. The powertrain model is part of the ECMS algorithm, which is an optimization-based operating strategy based on PMP. In order to apply the ECMS on the considered powertrain, an appropriate description of the Lagrange multiplier is required. Two methods for the determination of this description were presented: the Hamilton–Jacobi–Bellmann equation, which requires a predefined driving cycle and a corresponding optimization with DP in advance, and a control-based method, where the state of charge is controlled based on a predefined characteristic for the controller's setpoints. Both methods require a prediction of the future driving behavior. Either a driving cycle or the distance to be driven must be predicted. The analysis of the ECMS and its prediction methods was carried out based on various driving cycles, which were measured for the same route. For the predictions, either the mean driving cycle obtained from the measurements, the corresponding navigation data, or the distance to be driven was considered. As it turned out, the ECMS based the Hamilton–Jacobi–Bellmann equation enabled the best results. However, this method requires a driving cycle, which is usually unknown, and time-consuming optimization in advance. For the ECMS with the control-based approach, it is sufficient to know the distance to be driven. The fuel consumptions obtained with this method were higher compared with the ECMS based on the Hamilton–Jacobi–Bellmann equation but were still lower compared with a simple CD-CS operating strategy. The results of the analysis show that the ECMS enabled significant improvements in fuel consumption compared with a non-optimization-based method. It was found that, in general, the more information about the future driving behavior was available, the lower the fuel consumptions were.

The application of the ECMS is not limited to plug-in hybrid electric powertrains. It can also be applied to any other hybrid powertrain configuration which has one or more degrees of freedom regarding the control of the power distribution. Likewise, configurations without the capability of external recharging can be considered. The investigations conducted in this contribution can be carried out for other powertrain configurations, too. This will require a powertrain model in accordance with the considered configuration and an adaption of the ECMS's implementation to the corresponding control variables.

Author Contributions: Conceptualization, S.G.; methodology, S.G. and T.S.; writing–original draft preparation, S.G.; writing–review and editing, S.G., T.S. and J.M.; visualization, S.G.; supervision, T.S. and J.M. All authors have read and agreed to the published version of the manuscript.

Funding: This research was funded by the German Federal Ministry of Economics and Energy (BMWi) grant number (01MY13004B).

Data Availability Statement: The raw data supporting the conclusions of this manuscript will be made available upon request to T.S.

Acknowledgments: This contribution was accomplished within the project PHEVplus (FKZ: 01MY13004B), funded by the Federal Ministry of Economics and Energy (BMWi) and in cooperation with GKN Driveline International GmbH. The authors thank student Tobias Zubke for supporting this contribution.

Conflicts of Interest: The authors declare no conflict of interest.

References

1. Karbowski, D.; Pagerit, S.; Kwon, J.; Rousseau, A.; von Pechmann, K.-F.F. *"Fair" Comparison of Powertrain Configurations for Plug-In Hybrid Operation Using Global Optimization*; SAE Technical Paper; SAE: Detroit, MI, USA, 2009.
2. Brunner, M.; Fischer, R.; Küpper, K. Dedicated Hybrid Transmission (DHT)—A Solution for Increased Production Numbers of Hybrid Powertrains. In Proceedings of the FISITA World Automotive Congress, Busan, Korea, 26–30 September 2016.
3. Gassmann, T.; Aikawa, M. GKN Multi-Mode eTransmission for Premium Hybrid Vehicles. In Proceedings of the 12th International CTI Symposium, Berlin, Germany, 2–5 December 2013.
4. Kim, N.; Kwon, J.; Rousseau, A. *Comparison of Powertrain Configuration Options for Plug-In HEVs from a Fuel Economy Perspective*; SAE Technical Paper; SAE: Detroit, MI, USA, 2012.

5. Conlon, B.M.; Blohm, T.; Harpster, M.; Holmes, A.; Palardy, M.; Tarnowsky, S.; Zhou, L. The Next Generation "Voltec" Extended Range EV Propulsion System. *SAE Int. J. Altern. Powertrains* **2015**, *4*, 248–259. [CrossRef]
6. Grewe, T.M.; Conlon, B.M.; Holmes, A.G. *Defining the General Motors 2-Mode Hybrid Transmission*; SAE Technical Paper; SAE: Detroit, MI, USA, 2007.
7. Suenaga, S.; Yashsiro, T.; Sano, S.; Taniguchi, M.; Takizawa, K.; Baba, S.; Tsuchida, M.; Endo, H.; Kimura, H. Development of New Hybrid Transaxle for Compact Class Vehicles. In Proceedings of the FISITA World Automotive Congress, Busan, Korea, 26–30 September 2016.
8. Geng, S.; Meier, A.; Schulte, T. Model-Based Optimization of a Plug-In Hybrid Electric Powertrain with Multimode Transmission. *World Electr. Veh. J.* **2018**, *9*, 12. [CrossRef]
9. Wirasingha, S.G.; Emadi, A. Classification and Review of Control Strategies for Plug-In Hybrid Electric Vehicles. *IEEE Trans. Veh. Technol.* **2011**, *60*, 111–122. [CrossRef]
10. Malikopoulos, A.A. Supervisory Power Management Control Algorithms for Hybrid Electric Vehicles: A Survey. *IEEE Trans. Intell. Transp. Syst.* **2014**, *15*, 1869–1885. [CrossRef]
11. Liu, C.; Liu, Y. Energy Management Strategy for Plug-In Hybrid Electric Vehicles Based on Driving Condition Recognition: A Review. *Electronics* **2022**, *11*, 342. [CrossRef]
12. Wallentowitz, H.; Ludes, R. System control application for hybrid vehicles. In Proceedings of the IEEE International Conference on Control and Applications, Glasgow, UK, 24–26 August 1994.
13. Guzzella, L.; Sciarretta, A. *Vehicle Propulsion Systems—Introduction to Modeling and Optimization*, 2nd ed.; Springer: Berlin/Heidelberg, Germany, 2007.
14. Jalil, N.; Kheir, N.; Salman, M. A rule-based energy management strategy for a series hybrid vehicle. In Proceedings of the 1997 American Control Conference, Albuquerque, NM, USA, 4–6 June 1997.
15. Abdelsalam, A.A.; Cui, S. A Fuzzy Logic Global Power Management Strategy for Hybrid Electric Vehicles Based on a Permanent Magnet Electric Variable Transmission. *Energies* **2012**, *5*, 1175–1198. [CrossRef]
16. Lee, H.-D.; Sul, S.-K. Fuzzy-logic-based torque control strategy for parallel-type hybrid electric vehicle. *IEEE Trans. Ind. Electron.* **1998**, *45*, 625–632.
17. Schouten, N.J.; Salman, M.A.; Kheir, N.A. Energy management strategies for parallel hybrid vehicles using fuzzy logic. *Control Eng. Pract.* **2003**, *11*, 171–177. [CrossRef]
18. Lin, C.-C.; Peng, H.; Grizzle, J.; Kang, J.-M. Power management strategy for a parallel hybrid electric truck. *IEEE Trans. Control Syst. Technol.* **2003**, *11*, 839–849.
19. Bianchi, D.; Rolando, L.; Serrao, L.; Onori, S.; Rizzoni, G.; Khayat, N.A.; Hsieh, T.M.; Kang, P. Layered control strategies for hybrid electric vehicles based on optimal control. *Int. J. Electr. Hybrid Veh.* **2011**, *3*, 191. [CrossRef]
20. Biasini, R.; Onori, S.; Rizzoni, G. A near-optimal rule-based energy management strategy for medium duty hybrid truck. *Int. J. Powertrains* **2013**, *2*, 232. [CrossRef]
21. Van Berkel, K.; de Jager, B.; Hofman, T.; Steinbuch, M. Implementation of Dynamic Programming for Optimal Control Problems with Continuous States. *IEEE Trans. Control Syst. Technol.* **2015**, *23*, 1172–1179. [CrossRef]
22. Bertsekas, D.P. *Dynamic Programming and Optimal Control*, 3rd ed.; Athena Scientific: Belmont, MA, USA, 2005; Volume 1.
23. Moura, S.J.; Fathy, H.K.; Callaway, D.S.; Stein, J.L. A Stochastic Optimal Control Approach for Power Management in Plug-In Hybrid Electric Vehicles. *IEEE Trans. Control Syst. Technol.* **2011**, *19*, 545–555. [CrossRef]
24. Kim, N.; Cha, S.; Peng, H. Optimal Control of Hybrid Electric Vehicles Based on Pontryagin's Minimum Principle. *IEEE Trans. Control Syst. Technol.* **2011**, *19*, 1279–1287.
25. Tang, L.; Rizzoni, G.; Onori, S. Energy Management Strategy for HEVs Including Battery Life Optimization. *IEEE Trans. Transp. Electrif.* **2015**, *1*, 211–222. [CrossRef]
26. Chen, Z.; Xiong, R.; Wang, K.; Jiao, B. Optimal Energy Management Strategy of a Plug-in Hybrid Electric Vehicle Based on a Particle Swarm Optimization Algorithm. *Energies* **2015**, *8*, 3661–3678. [CrossRef]
27. Boehme, T.J.; Frank, B.; Schori, M.; Jeinsch, T. Multi-objective Optimal Powertrain Design of Parallel Hybrid Vehicles with Respect to Fuel Consumption and Driving Performance. In Proceedings of the European Control Conference (ECC), Strasbourg, France, 24–27 June 2014.
28. Boyd, S.; Vandenberghe, L. *Convex Optimization*; Cambridge University Press: Cambridge, UK, 2009.
29. Hadj-Said, S.; Colin, G.; Ketfi-Cherif, A.; Chamaillard, Y. Analytical Solution for Energy Management of Parallel Hybrid Electric Vehicles. *IFAC-PapersOnLine* **2017**, *50*, 13872–13877. [CrossRef]
30. Pham, T.H.; Kessels, J.T.B.A.; van den Bosch, P.P.J.; Huisman, R.G.M. Analytical Solution to Energy Management Guaranteeing Battery Life for Hybrid Trucks. *IEEE Trans. Veh. Technol.* **2016**, *65*, 1. [CrossRef]
31. Egardt, B.; Murgovski, N.; Pourabdollah, M.; Johannesson, L. Electromobility Studies Based on Convex Optimization: Design and Control Issues Regarding Vehicle Electrification. *IEEE Control Syst.* **2014**, *34*, 32–49.
32. Ngo, V.; Hofman, T.; Steinbuch, M.; Serrarens, A. Optimal Control of the Gearshift Command for Hybrid Electric Vehicles. *IEEE Trans. Veh. Technol.* **2012**, *61*, 3531–3543. [CrossRef]
33. Nüesch, T.; Elbert, P.; Flankl, M.; Onder, C.; Guzzella, L. Convex Optimization for the Energy Management of Hybrid Electric Vehicles Considering Engine Start and Gearshift Costs. *Energies* **2014**, *7*, 834–856. [CrossRef]

34. Panday, A.; Bansal, H.O. A Review of Optimal Energy Management Strategies for Hybrid Electric Vehicle. *Int. J. Veh. Technol.* **2014**, *2014*, 1–19. [CrossRef]
35. Sciarretta, A.; Guzzella, L. Control of hybrid electric vehicles. *IEEE Control Syst.* **2007**, *27*, 60–70.
36. Paganelli, G.; Guerra, T.M.; Delprat, S.; Santin, J.-J.; Delhom, M.; Combes, E. Simulation and assessment of power control strategies for a parallel hybrid car. *Proc. Inst. Mech. Eng. Part D J. Automob. Eng.* **2000**, *214*, 705–717. [CrossRef]
37. Sciarretta, A.; Back, M.; Guzzella, L. Optimal Control of Parallel Hybrid Electric Vehicles. *IEEE Trans. Control Syst. Technol.* **2004**, *12*, 352–363. [CrossRef]
38. Borhan, H.; Vahidi, A.; Phillips, A.M.; Kuang, M.L.; Kolmanovsky, I.V.; Cairano, S.D. MPC-Based Energy Management of a Power-Split Hybrid Electric Vehicle. *IEEE Trans. Control Syst. Technol.* **2012**, *20*, 593–603. [CrossRef]
39. Ngo, V.; Hofman, T.; Steinbuch, M.; Serrarens, A. Predictive gear shift control for a parallel Hybrid Electric Vehicle. In Proceedings of the 2011 IEEE Vehicle Power and Propulsion Conference, Chicago, IL, USA, 6–9 September 2011.
40. Mesbah, A. Stochastic Model Predictive Control an Overview and Perspectives for Future Research. *IEEE Control Syst. Mag.* **2016**, *36*, 30–44.
41. Serrao, L.; Onori, S.; Rizzoni, G. ECMS as a realization of Pontryagin's minimum principle for HEV control. In Proceedings of the 2009 American Control Conference, St. Louis, MO, USA, 10–12 June 2009.
42. Markel, T.; Brooker, A.; Hendricks, T.; Johnson, V.; Kelly, K.; Kramer, B.; O'Keefe, M.; Sprik, S.; Wipke, K. ADVISOR: A Systems Analysis Tool for Advanced Vehicle Modeling. *J. Power Sources* **2002**, *110*, 255–266. [CrossRef]
43. Naidu, D.S. Optimal Control Systems. In *Electrical Engineering Textbook Series*; CRC Press: Boca Raton, FL, USA, 2003.
44. Schori, M.; Boehme, T.J.; Frank, B.; Lampe, B.P. Optimal Calibration of Map-Based Energy Management for Plug-In Parallel Hybrid Configurations: A Hybrid Optimal Control Approach. *IEEE Trans. Veh. Technol.* **2015**, *64*, 3897–3907. [CrossRef]
45. Graphhopper: Open Source Routing Engine. 2020. Available online: www.graphhopper.com (accessed on 13 February 2022).